Journal of
Computational and Theoretical Nanoscience
Vol. 7, 1–5, 2010

Tunable Core Size of Carbon Nanoscrolls

Xinghua Shi[1,*], Nicola M. Pugno[2], and Huajian Gao[1]

[1] *Division of Engineering, Brown University, 610 Barus and Holley, Providence, RI 02912, USA*
[2] *Department of Structural Engineering, Politecnico di Torino, Corso Duca degli Abruzzi 24, 10129, Torino, Italy*

We study the equilibrium core radius of a carbon nanoscroll (CNS) formed from spontaneous rolling of a graphene sheet. By a balance between the elastic bending energy and the van der Waals interaction energy in the system, we derive an analytical relation between the surface energy, the bending stiffness, the interlayer spacing, the length of a graphene sheet and the core radius of the resulting CNS. This relation is then quantitatively verified by molecular dynamics simulations. Our work immediately suggests that the core size of a CNS can be actively controlled for applications such as tunable water and ion channels, molecular sensors, as well as flexible gene and drug delivery systems.

Keywords: Carbon Nanoscrolls, Molecular Dynamics, Core Size.

RESEARCH ARTICLE

Carbon nanoscralls (CNSs), also referred to as buckyrolls, may have numerous applications in nanotechnology due to their unique properties. So far most previous studies have been focused on carbon nanotube (CNT)-based nano- or nano-bio-systems, such as molecular probes or sensors,[1] gene or drug delivery systems.[2] Specifically, CNT–water,[3,4] CNT–CNT,[5] CNT–DNA oligonucleotides[6] and CNT–peptide[7] systems have been studied for encapsulating different types of molecules inside the CNTs. One disadvantage of the CNT-based systems is that the core size of CNTs is uncontrollable due to their closed structure. For applications such as tunable water and ion channels, molecular sensors, as well as flexible gene and drug delivery systems, it might be desirable to develop nanostructures with tunable core sizes. Here we show that carbon nanoscrolls may be a perfect candidate for such applications. Although CNSs were experimentally discovered in 2003[8,9] (see also Ref. [10]) and also investigated extensively by molecular dynamics simulations,[11–16] a quantitative theory describing their existence and assembly process is still unavailable. In the following, we present a theory on the dynamics and equilibrium state of this assembly process and show that the theoretical predictions are in excellent agreement with molecular dynamics simulations.

Figure 1(A) shows a graphene sheet of length B and width L rolled up into a scroll with inner core radius r_0, outer radius R and interlayer spacing t which can be described by a radial function as

$$r = r_0 + \frac{t}{2\pi}\vartheta \tag{1}$$

The total length of the graphene sheet is

$$B \approx \int_0^{2\pi N} \left(r_0 + \frac{t}{2\pi}\vartheta\right) \mathrm{d}\vartheta = 2\pi r_0 N + \pi t N^2 \tag{2}$$

where N is the number of coils. The elastic energy per unit area in the graphene is taken as

$$\frac{\mathrm{d}W}{\mathrm{d}A}(r) = \frac{D}{2}\frac{1}{r^2} \tag{3}$$

where D is the bending stiffness. Note that $\mathrm{d}A \approx Lr\mathrm{d}\vartheta$. The total elastic energy in the scroll is thus obtained by integrating Eq. (3) as

$$W = \frac{\pi DL}{t}\ln\left(\frac{R}{r_0}\right) \tag{4}$$

Consider an infinitesimal change in the core radius r_0 of the scroll. The change in strain energy would be

$$\mathrm{d}W = \frac{\pi DL}{t}\left(\frac{\mathrm{d}R}{R} - \frac{\mathrm{d}r_0}{r_0}\right) \tag{5}$$

It can be shown that

$$\frac{\mathrm{d}N}{\mathrm{d}r_0} = -\frac{N}{R}, \tag{6}$$

$$\frac{\mathrm{d}R}{\mathrm{d}r_0} = 1 + \frac{\mathrm{d}N}{\mathrm{d}r_0}t = 1 - \frac{Nt}{R} = \frac{r_0}{R}. \tag{7}$$

*Author to whom correspondence should be addressed.

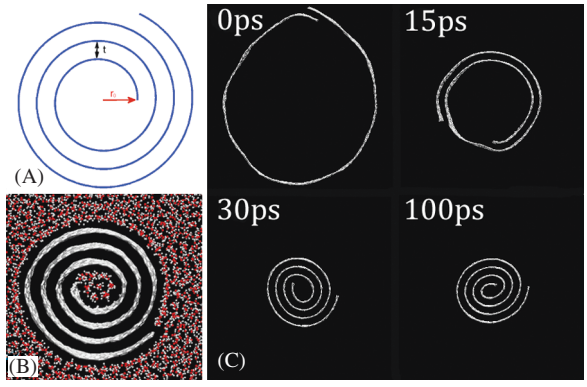

Fig. 1. (A) Buckyroll with inner core radius r_0 and interlayer spacing t. (B) Equilibrium core size in water. (C) MD snapshots on the spontaneous assembly of a zigzag graphene strip (3×24 nm^2) winding at 0, 15, 30, 100 ps.

Therefore, the change in elastic strain energy can be expressed as

$$dW = -\frac{\pi DL}{t}\frac{R^2 - r_0^2}{R^2}\frac{dr_0}{r_0} \tag{8}$$

On the other hand, the change in total surface energy of the scroll is

$$d\Gamma = 2\pi\gamma L(dr_0 + dR) = 2\pi\gamma L\left(1 + \frac{r_0}{R}\right)dr_0 \tag{9}$$

where γ is the surface energy per unit area. If the free energy of the system is assumed to be dominated by the elastic energy and surface (here mainly van der Waals) energy of the system, the virtual change in free energy associated with a "virtual core expansion" is

$$\frac{dE_{tot}}{dr_0} = \frac{dW}{dr_0} + \frac{d\Gamma}{dr_0} \tag{10}$$

The above equations show that, for very small core size, the strain energy dominates and there is a net driving force for core expansion. For very large core size, the surface energy dominates, and there is a net driving force for the system to contract. Therefore, a stable, equilibrium core size for the scroll can be calculated by setting $dE_{tot} = 0$, which yields

$$2\pi\gamma\left(1 + \frac{r_0}{R}\right) = \frac{\pi D}{t}\frac{R^2 - r_0^2}{R^2}\frac{1}{r_0} \tag{11}$$

Together with the mass conservation equation

$$B = \frac{\pi}{t}(R^2 - r_0^2) \tag{12}$$

the equilibrium core radius r_0 and the outer radius R of the scroll can be determined under fixed B, t, D, and γ.

The following relation shows how the surface energy, the bending stiffness, the interlayer spacing of graphene

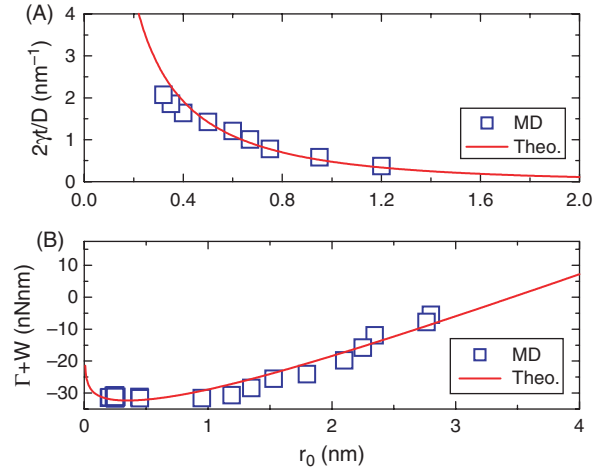

Fig. 2. (A) The ratio between surface energy and bending modulus of graphene as a function of the CNS core size; (B) The potential energy as a function of the core size. All results are obtained in vacuum. Blue squares are the MD results and red line is the theoretical prediction.

and the length of graphene sheet influence the core size of the CNS (Fig. 2(A))

$$\frac{2\gamma t}{D} = \frac{1}{r_0} - \frac{1}{\sqrt{(Bt/\pi) + r_0^2}} \tag{13}$$

Figure 2(B) plots the evolution of potential energy (elastic energy plus surface energy) as a function of the core size, which clearly indicates there is a stable equilibrium core size. The nearly constant slope of the red line shows that the driving force is almost constant before reaching the equilibrium.

Molecular dynamics (MD) simulations are performed and the results show that the assembly of buckyrolls occurs very fast (Fig. 1(C)). The equilibrium core size varies with different environment, large in water (Fig. 1(B)) and small in vacuum (Fig. 1(C)), for instance. The package Gromacs 4[17] is used here to simulate the formation of CNSs from a graphene sheet. The graphene is described by a Morse bond, a harmonic cosine term for the bond angle, a cosine term for torsion and a Lennard-Jones (L-J) term for the van der Waals (vdW) interaction as[18]

$$\begin{aligned} U(r_{ij}, \theta_{ijk}, \phi_{ijkl}) = {} & K_{Cr}[e^{-k_C(r_{ij}-r_C)} - 1]^2 \\ & + \frac{1}{2}K_{C\theta}(\cos\theta_{ijk} - \cos\theta_C)^2 \\ & + \frac{1}{2}K_{C\phi}(1 - \cos 2\phi_{ijkl}) \\ & + 4\varepsilon_{CC}\left[\left(\frac{\sigma_{CC}}{r_{ij}}\right)^{12} - \left(\frac{\sigma_{CC}}{r_{ij}}\right)^{6}\right] \end{aligned} \tag{14}$$

where k_C defines the steepness of Morse potential well, r_{ij} denotes distance between two bonded atoms, θ_{ijk} and ϕ_{ijkl} are the bending and torsional angle, r_C, θ_C and ϕ_C are the reference geometrical parameters for graphene, K_{Cr},

RESEARCH ARTICLE

Table I. Parameters of interaction potential used in the molecular dynamics simulations.

Interaction potential parameters[18]		
$K_{Cr} = 47890$ kJmol^{-1}nm^{-2}	$r_C = 0.142$ nm	$k_C = 21.867$ nm^{-1}
$K_{C\theta} = 562.2$ kJmol^{-1}	$\theta_C = 120^0$	
$K_{C\phi} = 25.12$ kJmol^{-1}	$\phi_C = 180^0$	
$\varepsilon_{CC} = 0.4396$ kJmol^{-1}	$\sigma_{CC} = 0.385$ nm	
$\varepsilon_{CO} = 0.529$ kJmol^{-1}	$\sigma_{CO} = 0.35$ nm	

$K_{C\theta}$ and $K_{C\phi}$ are the force constants of stretching, bending and torsion, respectively, and σ_{CC} and ε_{CC} are the L-J parameters for carbon. The spontaneous assembly of buckrolls are simulated in both vacuum and water. For the latter case, the graphene strips are solvated in a periodic $4 \times 10 \times 10$ nm orthorhombic box with Tip3p water.[19] The electrostatic interaction of water solvent is evaluated by the particle mesh Ewald method (PME).[20,21] The water–graphene interaction is described by the L-J potential with parameters $\sigma_{CO}$and ε_{CO}. Unless mentioned elsewhere, all the simulation parameters are listed in Table I. Room temperature (300 K) and atmospheric pressure (1 bar) are maintained in all simulations.

To investigate the effect of chirality on the buckyroll assembly, three deferent types of graphene strips, zigzag, armchair and chiral, are selected in the present simulations. To obtain the initial configuration shown in Figure 1(C) ($t = 0$ ps), external forces are initially applied to bring the two ends of a planar strip to a close vicinity. Thereafter the forces are removed and the system is set-free. The snapshots of the MD trajectory for a zigzag graphene (3×24 nm^2), shown in Figure 1(C), indicate that the graphene strip spontaneously winds into CNSs (see the movie, Supplementary material) and the winding process occurs very fast. The first loop is completed in $t = 15$ ps and three loops have already formed at $t = 30$ ps. After 50 ps, both the inner and outer radii have reached equilibrium, indicating the end of winding. The interlayer spacing is kept at a constant value 0.34 nm during the winding, exactly the same as that of the multiwalled carbon nanotube. The evolutions of the inner and outer radii are plotted in Figure 3(A), which indicates the speed of winding. To reveal the physical mechanism of the winding process, we plot the graphene–graphene interaction energy in Figure 3(B). At the initial state, the bending energy of the graphene is small because of the large radii. At this stage, the interaction energy dominates and drives the winding of the scroll. This process continues until the driving force is equivalent to the resistance force induced by the bending

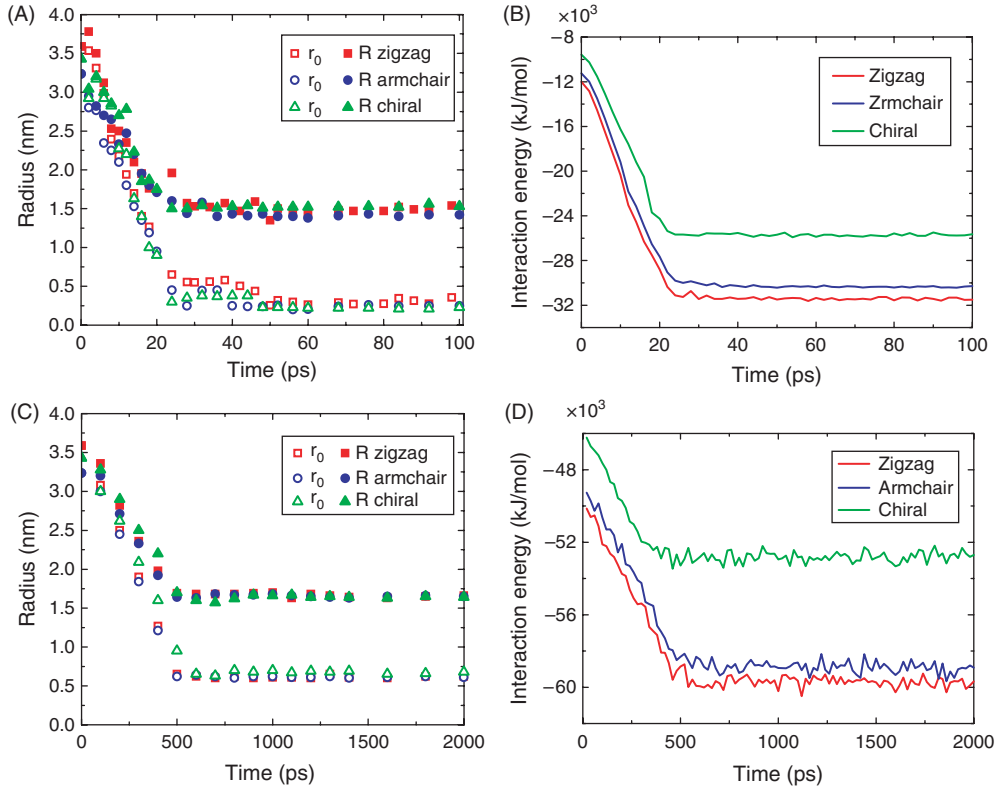

Fig. 3. (A) The simulated inner and outer radii of selected buckyrolls in vacuum as a function of the simulation time. Three types of graphene strips are simulated here: zigzag, armchair and chiral. (B) The simulated evolution of graphene–graphene interaction energy in vacuum as a function of time in the winding process. The steep slope at the initial state indicates that the surface energy of graphene is dominant. (C) The simulated inner and outer radii of selected buckyrolls in water as a function of the simulation time. (D) The simulated evolution of the total interaction energy as a function of time. Here the total interaction energy is taken to be the sum of graphene–graphene, water–water and graphene–water interaction energy.

RESEARCH ARTICLE

energy. To investigate the effect of graphene chirality, two additional graphene strips, armchair (3×24 nm^2) and chiral (2.4×23 nm^2), are used and the simulations are repeated. The similarly fast winding speed and the nearly same equilibrium core size suggest that the spontaneous winding of graphene is chirality independent. We also performed a simulation with a wider zigzag graphene strip (6×24 nm^2). The results are similar, indicating that the effect of scroll width is negligible.

In a box of water solvent, the winding process is slower because water molecules have to be squeeze out of the inner core in order for the winding process to complete. One interesting finding is that some water molecules remain inside the inner core even at equilibrium and the water molecules also form a spiral roll similar to the graphene sheet (Fig. 1(B)). This phenomenon is attributed to the confinement of the inner core and the finding that the structure of encapsulated water mimics that of the confining graphene structure is similar to the previous study on water structure confined in carbon nanotubes.[3]

To aid theoretical calculations on the core size of buckyrolls, we adopt a simple method to determine the bending modulus D of graphene. We calculate the strain energy of a series of carbon nanotubes with different radii. With the force field used in the present work, the relation between the strain energy per unit area and the tube radius is plotted in Figure 4. With the definition of bending energy

$$E_{\text{bending}} = \frac{1}{2} D \frac{1}{R^2} \tag{15}$$

we obtain the bending modulus of graphene $D = 0.11$ nN$\cdot$nm, in excellent agreement with results in the literature.[22] To find the surface energy γ, we plot the interaction energy versus the size of the buckyroll. According to the Eq. (9) the increment of interaction energy is a linear function of the increment of $r_0 + R$ with a slope of $2\pi\gamma L$. Therefore, the slope in Figure 5 (green line) corresponds to

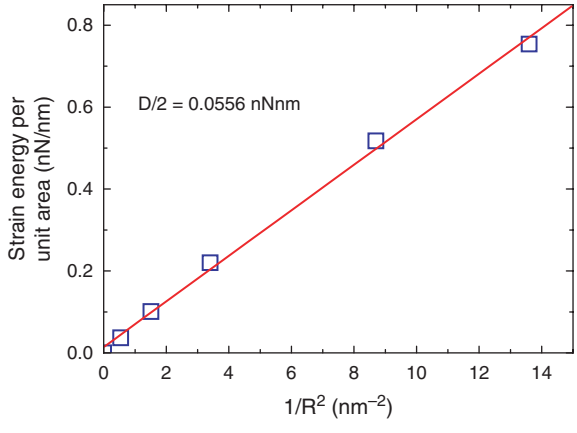

Fig. 4. The elastic strain energy of a carbon nanotube as a function of its radius. Blue squares are the molecular simulations results and red line is the linear fitting. The slope of the red line is half of the bending modulus.

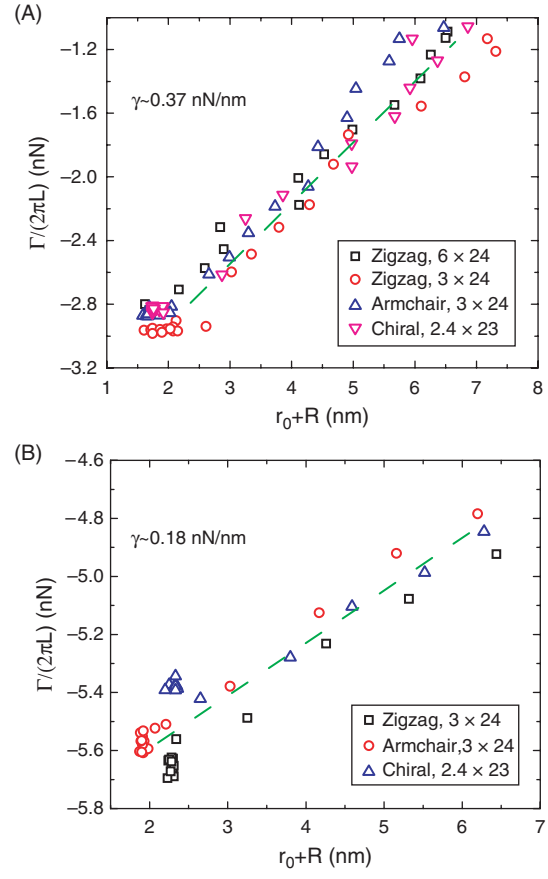

Fig. 5. (A) The interaction energy of buckyrolls in vacuum as a function of their size. Four different kinds of graphene are simulated with results indicating that the surface energy is about 0.37 nN/nm. (B) The total interaction energy of buckyrolls in water as a function of their size. The results provide an estimate of the surface energy of graphene in water to be about 0.18 nN/nm.

the surface energy. The interaction energy of a buckyroll in water solvent consists of three parts: graphene–graphene, water-water and graphene–water interactions. The surface energy of graphene in water is reduced to about half its value in vacuum. The simulated equilibrium configurations for different types of CNSs are in excellent agreement with the corresponding theoretical predictions (Table II). The simulations also show a constant contraction speed of CNSs in approaching their equilibrium core size (see the movie, Supplementary material). This phenomenon is consistent with a viscous damping process under a constant driving force,

$$-\frac{\mathrm{d}(W+\Gamma)}{\mathrm{d}r_0} = c(T)\dot{r}_0 \tag{16}$$

where $c(T)$ is the damping coefficient, which depends on the temperature of the system.

In conclusion, the core size of CNSs can be controlled by several different ways. Eq. (13) shows that the surface energy of CNSs directly determines the core size.

RESEARCH ARTICLE

Table II. Comparison between predicted (Theo.) and simulated (MD) equilibrium configurations of buckyrolls of different types.

	r_0 (nm)		R (nm)	
Theo/MD comparison	MD	Theo.	MD	Theo.
Zigzag$^{(v)a}$	0.32	0.37	1.50	1.65
Armchair$^{(v)}$	0.25	0.36	1.42	1.64
Chiral$^{(v)}$	0.23	0.33	1.56	1.61
Zigzag$^{(w)}$	0.60	0.59	1.59	1.7
Armchair$^{(w)}$	0.61	0.56	1.60	1.68
Chiral$^{(w)}$	0.68	0.79	1.67	1.73
Zigzag$^{(v,\,halfvdW)b}$	0.67	0.63	1.76	1.73

^{a}(v) means in vacuum and (w) means in water, ^{b}50% reduction in van der Waals interaction.

Base on the finding that electric field would induce polarizable carbon atoms of CNTs[23] and dipole molecule on surface would influence its surface energy,[24] through electric field, we may control the core size of CNSs by changing the effective surface energy. Equation (13) also shows that the length of graphene influences the core size of CNSs. So it is desirable to design CNSs with different core size by selecting graphenes with different length. We may also control the core size by pressure or mechanical force and functionalization of CNSs. Such tunable CNSs may have enormous potential in the applications such as nanopore sequencing of DNA,[25] controllable water and ion channels[3, 4, 26] and gene or drug delivery systems.[2, 6, 7]

References

1. P. Avouris, *Acc. Chem. Res.* 35, 1026 **(2002)**.
2. L. Lacerdaa, A. Biancob, M. Pratoc, and K. Kostarelosa, *Adv. Drug Deliv. Rev.* 58, 1460 **(2006)**.
3. G. Hummer, J. C. Rasalah, and J. P. Noworyta, *Nature (London)* 414, 188 **(2001)**.
4. F. Zhu and K. Schulten, *Biophys. J.* 85, 236 **(2003)**.
5. J. Zou, B. Ji, X. Q. Feng, and H. Gao, *Nano Lett.* 6, 430 **(2006)**.
6. H. Gao, Y. Kong, D. Cui, and C. S. Ozkan, *Nano Lett.* 3, 471 **(2003)**.
7. G. R. Liu, Y. Cheng, D. Mi, and Z. R. Li, *Int. J. Mod. Phys. C* 16, 1239 **(2005)**.
8. H. Shioyama and T. Akita, *Carbon* 41, 179 **(2003)**.
9. L. M. Viculis, J. J. Mack, and R. B. Kaner, *Science* 299, 1361 **(2003)**.
10. M. V. Savoskin, V. N. Mochalin, A. P. Yaroshenko, N. I. Lazareva, T. E. Konstantinova, I. V. Barsukov, and I. G. Prokofiev. *Carbon* 45, 2797 **(2007)**.
11. Y. Chen, J. Lu, and Z. Gao, *J. Phys. Chem. C* 111, 1625 **(2007)**.
12. R. Rurali, V. R. Coluci, and D. S. Galvão, *Phys. Rev. B* 74, 085414 **(2006)**.
13. S. F. Braga, V. R. Coluci, S. B. Legoas, G. Giro, D. S. Galvão, and R. H. Baughman, *Nano Lett.* 4, 881 **(2004)**.
14. S. F. Braga, V. R. Coluci, R. H. Baughman, and D. S. Galvão, *Chem. Phys. Lett.* 441, 78 **(2007)**.
15. V. R. Coluci, S. F. Braga, R. H. Baughman, and D. S. Galvão, *Phys. Rev. B* 75, 125404 **(2007)**.
16. G, Mpourmpakis, E. Tylianakis, and G. E. Froudakis, *Nano Lett.* 7, 1893 **(2007)**.
17. B. Hess, C. Kutzner, D. van der Spoel, and E. Lindahl, *J. Chem. Theory Comput.* 4, 435 **(2008)**.
18. J. H. Walther, R. Jaffe, T. Halicioglu, and P. Koumoutsakos, *J. Phys. Chem. B* 105, 9980 **(2001)**.
19. W. L. Jorgensen, J. Chandrasekhar, J. D. Madura, R. W. Impey, and M. L. Klein, *J. Chem. Phys.* 79, 926 **(1983)**.
20. T. Darden, D. York, and L. Pedersen, *J. Chem. Phys.* 98, 10089 **(1993)**.
21. U. Essmann, L. Perera, M. L. Berkowitz, T. Darden, H. Lee, and L. G. Pedersen, *J. Chem. Phys.* 103, 8577 **(1995)**.
22. D. W. Brenner, O. A. Shenderova, J. A. Harrison, S. J. Stuart, B. Ni, and S. B. Sinnott, *J. Phys.: Condens. Mat.* 14, 783 **(2002)**.
23. R. Langlet, M. Devel, and P. H. Lambin, *Carbon* 44, 2883 **(2006)**.
24. R. Maheshwari, R. Parthasarathi, and A. Dhathathreyan, *J. Col. Int. Sci.* 271, 419 **(2004)**.
25. A. Meller, L. Nivon, E. Brandin, J. Golovchenko, and D. Branton, *Proc. Natl. Acad. Sci. USA* 97, 1079 **(2000)**.
26. J. Y. Li, X. J. Gong, H. J. Lu, D. Li, H. P. Fang, and R. H. Zhou, *Proc. Natl. Acad. Sci. USA* 104, 3687 **(2007)**.

Received: 30 March 2009. Accepted: 25 April 2009.